

Automated Diagnosis of Material Condition in Hammering Test Using a Boosting Algorithm

Hiromitsu Fujii¹, Atsushi Yamashita¹ and Hajime Asama¹

Abstract—Automated diagnosis systems are necessary for the maintenance of superannuated social infrastructure. This paper presents a methodology for detecting material defects using acoustic signals in a hammering test. The approach comprises a feature extraction step using Short-Time Fourier Transform (STFT) and a classifier training step based on AdaBoost, an ensemble learning algorithm. Especially, we use weak learners based on a simple template matching method that can consider both the variable scale of amplitude and the variable frequency band. The experiments discriminate between defective and clean materials using different hammering test methods: *rubbing* and *tapping*.

I. INTRODUCTION

In recent years, superannuation of social infrastructure has become a major problem involving installations such as tunnels and bridges built during Japan’s rapid economic growth era. Early detection of problems by continuous inspection of that infrastructure is indispensable. However, a huge amount of infrastructure needs inspection [1]. Moreover, the locations to be inspected, such as high and narrow places, are dangerous for workers in many cases. It is extremely difficult to inspect all of them manually. Therefore, development of an automated inspection system, such as one using robots, is strongly desired.

At equipment inspection sites, visual diagnosis and percussion diagnosis (Fig. 1) have been widely used. Particularly percussion diagnosis is mainly adopted because of its high accuracy and ease of execution. However, manual diagnosis relies on personal skill. Much experience is necessary for accurate diagnosis. Furthermore, skilled inspectors are decreasing in number because of their retirement age. Development of automated diagnosis methods that can be executed quickly, accurately and easily is urgently in demand.

Although many studies of diagnostic systems of infrastructure inspection have been made, such systems are not efficient enough because most of these are manual system depending on visual inspection by remote operators. However, automated hammering test robots have been developed, such as one which detects cavities from inner walls of concrete tunnels [2] and one which detects tile exfoliations from outer walls of high-rise buildings [3]. However, these robots are difficult to install and use because they are large-scale systems and their diagnostic methods have not become automated enough. BETOSCAN [4], a sensor equipped in compact robotic systems, can detect corrosion in reinforced

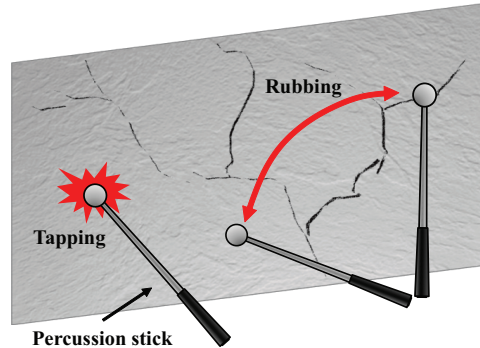


Fig. 1. Hammering test (*rubbing* and *tapping*).

concrete decks. Nevertheless, automation of diagnostic processes is limited to specific problems when the diagnosis is based on detailed analysis of a material or a structure. This limitation is common among numerous inspection systems.

A considerable number of proposed automated diagnostic techniques for infrastructure are based on image processing [5], [6] or machine learning methodologies such as Support Vector Machine [7] and Neural Networks [8]. As one example of acoustic diagnosis, a diagnostic decision-support system of concrete pipelines was developed by Iyer *et al.* [8]. The study used ultrasonic signals and presented a methodology based on Multi-Layer Neural Network to detect multi-modal defects such as holes and cracks of various sizes. Although these methodologies can support human work such as walk-around checks, they are insufficient from the perspective of automation of huge-scale inspections. These facts underscore the necessity of a methodology that can diagnose defects quickly, precisely, and automatically.

As described in this paper, a proposed methodology can construct a classifier adaptively to detect defects for a diagnosis. We specifically examine a hammering test, which provides an accurate diagnosis with ease of execution. A method of extracting feature vectors from acoustic signals obtained in the test and a method of construction of classifiers based on a boosting algorithm are presented. Using crack detection experiments, we verify the proposed method.

II. AUTOMATED DIAGNOSTIC METHOD

A. Hammering Test

Hammering tests using a special stick or a hammer, called a percussion stick, are widely used for inspection work. The diagnostic tests include several methods such as *rubbing* by the sound of stroking on the material surface or *tapping* by the sound of hitting, as shown in Fig. 1. Both of these

¹H. Fujii, A. Yamashita and H. Asama are with the Department of Precision Engineering, Faculty of Engineering, The University of Tokyo, 7-3-1 Hongo, Bunkyo-ku, Tokyo 113-8656, Japan. {fujii, yamashita, asama}@robot.t.u-tokyo.ac.jp

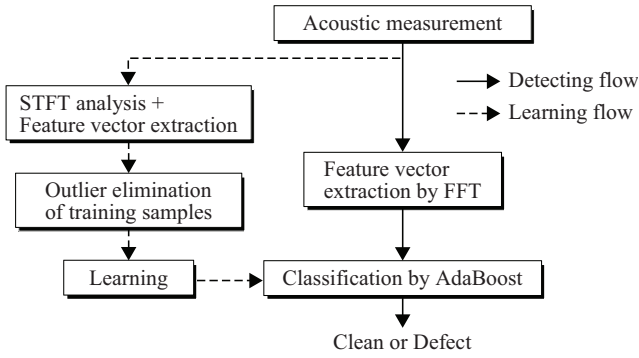


Fig. 2. Proposed method for defect detection.

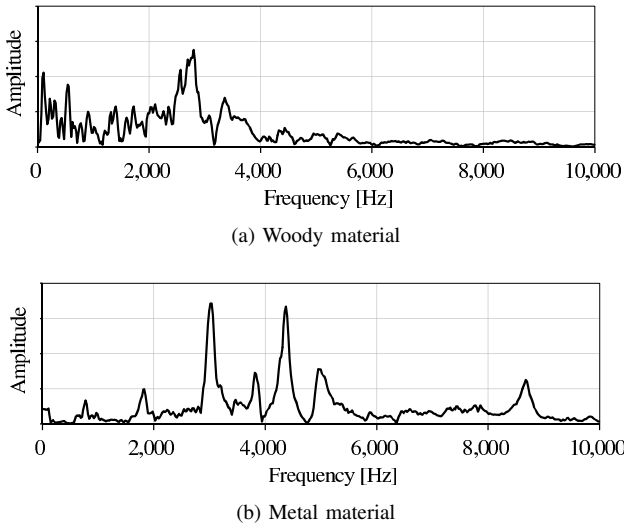


Fig. 3. Hammering test spectrum examples.

diagnostic methods use acoustic features to detect material defects. Although skilled techniques are necessary for acoustic diagnosis, a hammering test is commonly applied because of its accuracy. At current inspection sites, selecting diagnostic methods according to the situation is necessary. Therefore, in this study, we propose a defect detection method using acoustic signals obtained from both *rubbing* and *tapping*.

B. Approach to Defect Detection

The overall scheme of defect detection in the approach of this study is presented in Fig. 2. The procedure of constructing a classifier, shown as *Learning flow* in Fig. 2, consists of three steps. First, input acoustic signals in time series are transformed to the frequency domain by Short-Time Fourier Transform (STFT). A frequency spectrum is treated as a feature vector. Second, each feature vector is verified and eliminated if detected as an outlier. Finally, a classifier is constructed based on the AdaBoost algorithm, which is a kind of supervised learning under ensemble learning methods.

1) *Extraction of Feature Vector using STFT*: Fourier transform (FT) has been commonly applied to signal processing to convert a time series into a frequency domain. STFT

is a method of time-frequency transformation. The method has been used for machine faults detection or nondestructive inspection of infrastructures [9], [10], [11]. Signals are multiplied by a window function sliding along the time axis and transformed by FT so that the resulting signal can be analyzed in a time-frequency dimensional representation. For this study, recorded acoustic signals are converted by STFT using a Hanning window function. The resulting signals are taken as a set of feature vectors that represent conditions of an inspection target.

For example, differences of feature vectors between woody materials and metal ones are shown respectively in Fig. 3(a) and Fig. 3(b). In both figures, the horizontal axis shows frequency; the vertical axis shows signal amplitude in the frequency domain. In this case, the sampling frequency is 44.1kHz and the number of data samples for FFT is 2,048. Although both two materials are in the similar plate shape, a comparison between Fig. 3(a) and Fig. 3(b) shows that these feature vectors differ. In particular, the amplitude of high frequency components in metal materials is larger than that in woody materials. The classifiers in this study use such frequency domain features to detect defects in materials.

2) *Outlier Elimination in Training Samples*: Although ensuring consistency of the sample set is important to construct a precise classifier in supervised learning, training samples can include contradictory data because of noise in the measuring environment. Consequently, a preprocessing procedure that eliminates outliers in the measured data as contradictory data is conducted.

All feature vectors are standardized to avoid scale effects of sound pressure. Outliers are detected and removed based on the dispersion of data in a standardized feature space. The procedure is the following. An average of feature vectors (known as center of gravity) from each signal source is calculated. Assuming that the distribution of the distance between each feature vector and the center of gravity obeys a normal distribution, then the data which exist outside 3σ can be eliminated as outliers, where σ is the standard deviation of the distance.

3) *Classifier Construction by AdaBoost*: This subsection briefly describes the basis for classifier construction based on AdaBoost. Our approach of detecting defects in various materials is also presented.

AdaBoost, an ensemble learning algorithm [12], is known as a representative boosting algorithm, which is a machine learning meta-algorithm to create a strong learner by integrating a set of weak learners. In a boosting algorithm, as shown in Fig. 4, the whole learner (strong learner) consists of plural learners (weak learners). The strong learner combines outputs of the weak learners using a weighted majority vote. Each weak learner is created in order with updating of the weights of training samples. The training samples that a previous weak learner misclassified are weighted in the next learning step, so that the weak learner in later steps can emphasize the process of distinguishing data that are difficult to classify. Based on the characteristics, it seems reasonable to infer that this framework of learning is suitable

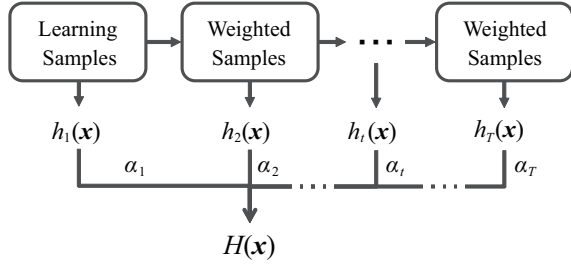


Fig. 4. Schematic view of a general boosting algorithm.

for application to material diagnostic problems that include defects that are difficult to detect. In this study, we refer to the algorithm of Viola *et al.* [13].

In the AdaBoost algorithm, the strong learner $H(\mathbf{x})$ for a feature vector \mathbf{x} is a binary classifier as

$$H(\mathbf{x}) = \text{sign} \left[\sum_{t=1}^N \alpha_t h_t(\mathbf{x}) \right] \in \{-1, 1\}, \quad (1)$$

where $h_t(\mathbf{x})$ is a weak learner in learning step t . N is the number of weak learners that organize a strong learner. α_t is confidence of each weak learner computed by the error ratio ϵ_t of classification of training samples as

$$\alpha_t = \log \left(\frac{1 - \epsilon_t}{\epsilon_t} \right), \quad (2)$$

such that $\epsilon_t \leq 0.5$ and $\alpha_t \geq 0$ are always satisfied in binary classification. The error ratio ϵ_t of the weak learner $h_t(\mathbf{x})$ is obtained by testing all training samples $\{\mathbf{x}^{(i)}\}$ with $h_t(\mathbf{x})$. The subscript i is the index of training samples, for the i -th set of training samples $\mathbf{x}^{(i)}$, the weights $w_t^{(i)}$ of $\mathbf{x}^{(i)}$ are updated at the end of learning step t as

$$w_{t+1}^{(i)} = w_t^{(i)} \left(\frac{\epsilon_t}{1 - \epsilon_t} \right)^{1 - e^{(i)}}, \quad (3)$$

where $e^{(i)}$ is the variable which indicates the result of classification. Setting $e^{(i)} = 0$ if example $\mathbf{x}^{(i)}$ is classified correctly, $e^{(i)} = 1$ otherwise. At the beginning of each learning step, $w_t^{(i)}$ is normalized as

$$\sum_i w_t^{(i)} = 1. \quad (4)$$

As a result, the weights of misclassified training samples would be increased in the next learning step.

The amplitude scale of feature vectors can vary according to the impact strength when hit in the hammering test. The available frequency band for diagnosis differs by material to be inspected. The weak learner we propose can classify signals robustly without being affected by these effects, using a template matching function based on Normalized Cross-Correlation $S_t(\mathbf{T}_t, \mathbf{x})$:

$$S_t(\mathbf{T}_t, \mathbf{x}) = \frac{\sum_{k \in \mathcal{K}} (T_t(k) - \bar{T}_t)(x(k) - \bar{x})}{\sqrt{\sum_{k \in \mathcal{K}} (T_t(k) - \bar{T}_t)^2} \sqrt{\sum_{k \in \mathcal{K}} (x(k) - \bar{x})^2}}, \quad (5)$$

where \mathbf{T}_t is the template vector calculated with feature vectors of training samples in learning step t . \bar{T}_t and \bar{x} respectively denote the average value of \mathbf{T}_t and \mathbf{x} . The set \mathcal{K} , the details of which are described later, represents the frequency band used in classification of \mathbf{x} . The index k denotes each frequency component of \mathcal{K} .

The $S_t(\mathbf{T}_t, \mathbf{x})$ evaluates similarity between the template vector \mathbf{T}_t and input vector \mathbf{x} . Using $S_t(\mathbf{T}_t, \mathbf{x})$, the classification of \mathbf{x} by each weak learner $h_t(\mathbf{x})$ is

$$h_t(\mathbf{x}) = \begin{cases} 1 & \text{if } S_t(\mathbf{D}_t, \mathbf{x}) - S_t(\mathbf{C}_t, \mathbf{x}) > \theta \\ -1 & \text{otherwise} \end{cases}, \quad (6)$$

where θ is the threshold for classification to be designed for each learner, which is also described later. \mathbf{D}_t is the template vector created by the training samples obtained from defect materials, \mathbf{C}_t is one from clean materials. Both of the template vectors are calculated considering the weights $w_t^{(i)}$ for training samples $\mathbf{x}^{(i)}$ as

$$\mathbf{D}_t(k) = \sum_{i \in \mathcal{N}_D} w_t^{(i)} x^{(i)}(k), \quad (7)$$

$$\mathbf{C}_t(k) = \sum_{i \in \mathcal{N}_C} w_t^{(i)} x^{(i)}(k), \quad (8)$$

where \mathcal{N}_D is the defect class, which is the set of indices of training samples obtained from defect materials, and \mathcal{N}_C is the clean class. That is to say, $\mathbf{x}^{(i)}$ belongs to the defect class if $i \in \mathcal{N}_D$, and $\mathbf{x}^{(i)}$ belongs to the clean class if $i \in \mathcal{N}_C$.

In (5) and (6), \mathcal{K} and θ are the parameters which ought to be designed for each weak learner. \mathcal{K} is the frequency band in which \mathbf{x} is compared with the template vector. It represents the feature vector space. \mathcal{K} is optimized simultaneously while learning each weak classifier because the features of acoustic signals vary according to the health condition or kind of material. Optimization of \mathcal{K} can construct the adaptive classifier to each diagnostic problem. Variable θ is the threshold which determines the result of classification by the balance between Normalized Cross-Correlation function values. \mathcal{K} and θ for the weak learner of each learning step are selected so that the error ratio ϵ_t is minimized. ϵ_t is evaluated repeatedly in trials where the plural candidates of a weak learner, which are given the parameters randomly, respectively classify all training samples.

In this way, a new evaluation sample \mathbf{x} is classified using a majority vote by the plural weak learners $h_t(\mathbf{x})$, which are weighted by their own confidence α_t , as shown in (1). That is to say, the defect samples are classified in *Class D* where $H(\mathbf{x}) = 1$, and the clean samples are classified in *Class C* where $H(\mathbf{x}) = -1$.

III. METHOD EVALUATION

The applicability of the proposed method to various methods in the hammering test was tested by experimentation. In this section, experiments with *rubbing* inspection (Section III-A) and *tapping* inspection (Section III-B) are presented.

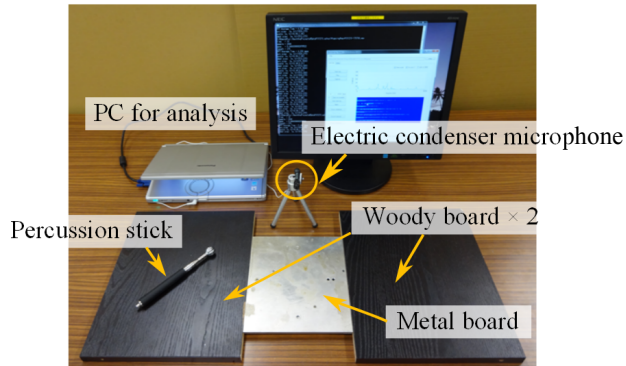


Fig. 5. Experimental environment of crack detection with rubbing.

A. Laboratory Experiment of Crack Detection with Rubbing

1) *Experimental Setting*: Experimental equipment is shown in Fig. 5. We used a plywood board and stainless plate as the inspection materials. The device for recording was an electric condenser microphone with resolution and sampling rate, respectively, of 16bit and 44.1kHz.

In the experiment, the number of samples for FFT were 2,048. A Hanning window function was applied. The number of weak classifiers was set as 100. The parameters \mathcal{K} and θ were designed as described below. For the frequency band \mathcal{K} , the lower bound was fixed to 50Hz. The upper bound was variable in the range of 5,000Hz to 10,000Hz, in which the material condition appears clearly. The dimensions of feature vectors alter depending on the scale of frequency band. Letting the threshold θ be variable in the range $0 < \theta < 1.0$, both parameters were optimized in each range as described above.

2) *Experimental Results and Discussion*: For verifying the precision of the proposed method, a basic experiment of crack detection in woody materials was conducted by a *rubbing* inspection. The experimental setting is shown in Fig. 6, where a pseudo-crack was set by fixing two plywood boards 3mm apart on the floor. The training samples in this experiment are shown in Table I. *Class D* consisted of feature vectors obtained from rubbed sounds at the moment of passing on the crack. A sample x in the dataset ought to be detected: $H(x) = 1$. However, *Class C* consisted of feature vectors obtained from the environmental sound of various sources such as a clean rubbed, a metal rubbed, footsteps, and an air conditioner. A sample x in the dataset ought not to be detected: $H(x) = -1$.

The performance of the classifier was evaluated using K -fold cross-validation. Letting the subsample size K be 10, the classifier accuracy was 98.1% for *Class D* and 98.6% for *Class C*. The average of training time was 356s on a desktop computer (Intel Core™ i7-4770 CPU (3.40GHz)).

The detection result is shown in Fig. 7. The evaluation sample was measured distinctly from training samples. In Fig. 7(a), the result in the time domain is shown: the horizontal axis shows time [ms]; the vertical axis shows the microphone input amplitude. Fig. 7(b) is the spectrogram in

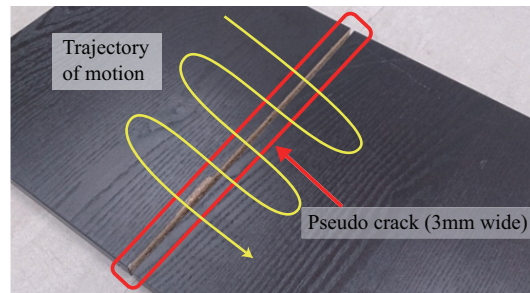


Fig. 6. Pseudo-crack in woody boards

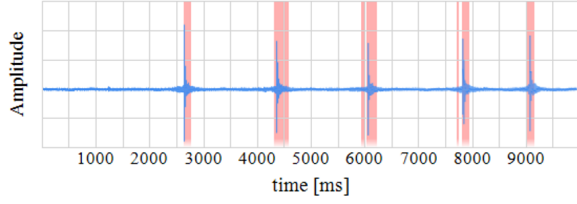
Table I
TRAINING SAMPLES OF RUBBING TESTS.

Class	Learning sample	Number of samples
<i>Class D</i>	rubbed sound at the moment of passing on the crack	1,405
<i>Class C</i>	rubbed sound of plywood and stainless, and environmental sound	1,476

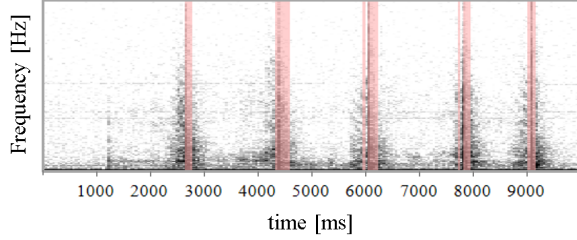
the time–frequency domain: the horizontal axis shows time [ms]; the vertical axis shows frequency [Hz] between 50Hz and 10,000Hz. The shades of colors represent amplitudes of the frequency spectrum. A deeper color denotes the larger amplitude. In this experiment, the materials were rubbed, making five round trips between two boards during 10,000ms. The trajectory of the motion is shown in Fig. 6. From sharp peaks of microphone input in Fig. 7(a), the moments of impacts passing on the crack is confirmed, for example the woody board was tapped at the moment roughly between 2,500ms and 2,750ms.

In both Fig. 7(a) and Fig. 7(b), the areas emphasized by a half-tone background indicated the time zones that were detected as the rubbed sounds of the crack were 2,600ms–2,750ms, 4,300ms–4,600ms, 5,900ms–6,200ms, 7,700ms–7,900ms and 9,000ms–9,200ms. These time zones coincided well with the moment of passing on the crack of the board.

Although the moments of rubbing clean parts and doing nothing were classified correctly, a few moments of rubbing defective parts were classified incorrectly as those of clean parts. It is possible that the misclassification in this case resulted from the difference of the motion velocity between training samples and evaluation samples. Rapid rubbing motions produce an increase of the amplitude of high-frequency components in the measured sound, so that the similarity to the template vector will decrease. The proposed evaluation function shown in (5) can accommodate the variable scale of amplitude, but it cannot cope with the shift of spectrum caused by a difference of motion velocity. Although a problem of this kind is not so important because sudden deceleration or acceleration is improbable in an inspection done by robots, we presume that taking advantage of additional information such as velocity or vision is useful to improve the classifier accuracy.



(a) Crack detection result in the time domain



(b) Crack detection result in the frequency domain

Fig. 7. Cracks detection results in woody materials.

3) *Results of Learning*: The relation between the number of the weak learners and the classifier accuracy are shown in Fig. 8. The horizontal axis shows the learning step count, which equals the number of weak learners. The vertical axis shows the average error ratio as evaluated by ten-fold cross-validation, which is expressed as a percentage. The result confirmed that the increase of the number of the weak learners produced the decrease of the error ratio, so that the effectiveness of integrating plural learners for the diagnostic problem was stated. In each learning step of AdaBoost, the weight $w_t^{(i)}$ for the training sample $\mathbf{x}^{(i)}$, which is difficult to classify, is weighted more in the next step according to (3). The weights of training samples in the last learning step ($t = 100$) are shown in Fig. 9. The horizontal axis shows the identifiers of training samples. The vertical axis shows the weight sample $w_{100}^{(i)}$ of each. Some samples weighted in the last phase of the learning step were difficult to classify. For example, if the environmental sound of measurement spot included the specific frequency components in a wide range, then both classes were mutually similar in the feature space. These results indicate that the proposed methodology can produce a robust classifier adaptively for difficult diagnostic problems.

B. Crack Detection on Gypsum Wall with Tapping

An experiment of crack detection on the wall of gypsum board using *tapping* inspection was conducted. Gypsum board is widely used as an office building material. Wall deterioration is pointed out as the cause of secondary disaster in earthquakes because it is used for furniture fixing in spite of its fragility. Based on this fact, automated crack detection on a gypsum wall is useful to forecast the progress of deterioration.

1) *Environmental Settings*: Locations of cracks in the gypsum wall were detected using the *tapping* method. The

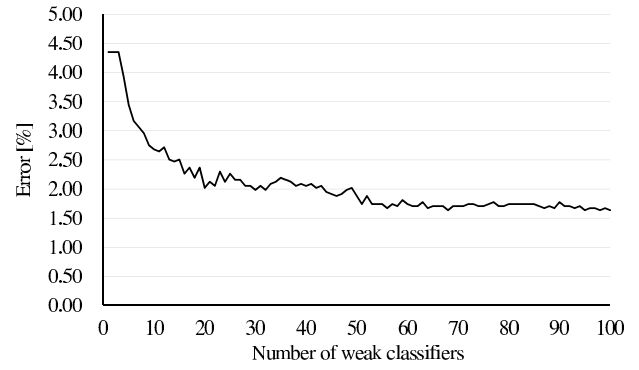


Fig. 8. Error of training results in cross validation.

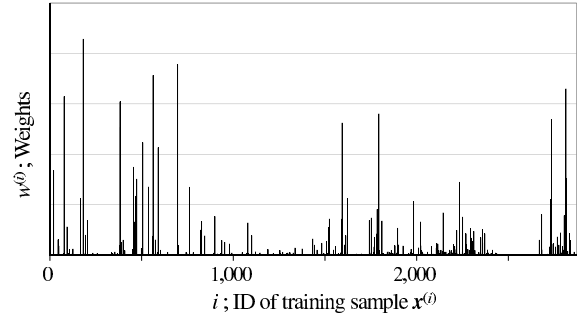


Fig. 9. Final weights of training samples in the crack detection test.

experimental environment is shown in Fig. 10(a). The devices were a microphone for recording tapping sounds and a camera for detecting the locations of hit positions. The microphone and the camera were fixed at a position 500mm distant in front of the wall, the camera direction was perpendicular to the wall surface. A region of interest for inspection is shown in Fig. 10(b). Letting the horizontal axis and vertical axis be X-axis and Y-axis, respectively, the inspection area was as follows: 500mm in the X-axis direction, 340mm in the Y-axis direction. As shown in Fig. 10(c), the area was segmented into 8×8 small areas. The camera resolution was 640×480 pixels, so that each small area was roughly 55mm and 40mm in the X-axis and the Y-axis direction. By *tapping*, the small areas were inspected one-by-one to discriminate the existence of cracks in the area. A hit position was identified by detecting the head of the percussion stick, which is marked in red, using an image-processing technique.

In buildings, hammering test sounds vary by location because of existence of various materials in the other side of the wall, such as diagonal beams and pipes spaces. Therefore, it is likely that sound spectrum of clean wall can alter by the location. For this reason, training samples were measured at plural locations, which differed from the evaluation samples tested in Section III-B.2. The training samples are shown in Table II. *Class D* included feature vectors obtained from tapping sounds of defective walls. On the other hand, *Class C-1*, *C-2* and *C-3* included other feature vectors that ought not to be detected. They were obtained from the three kind of clean walls. *Class C-1* was the set of samples of the walls which were shared with the

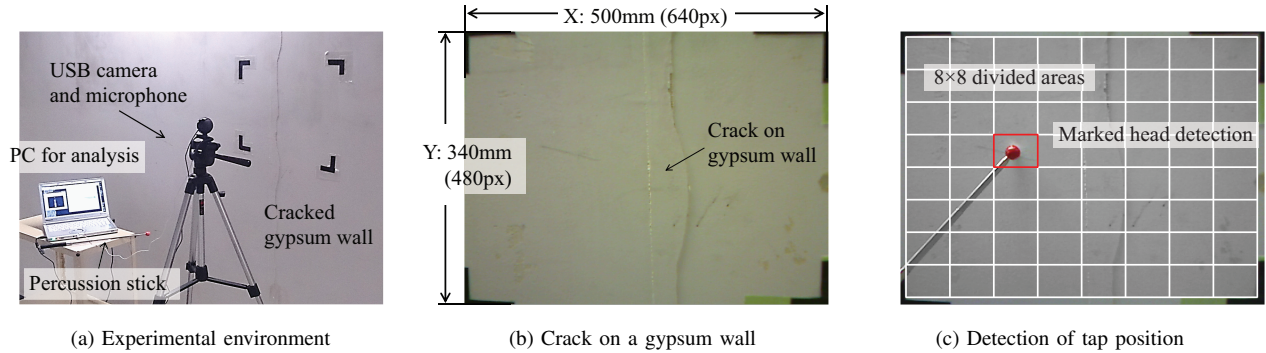


Fig. 10. Experimental environment for crack detection on the gypsum wall.

Table II
LEARNING SAMPLES FOR CRACK DETECTION ON WALLS.

Class	Learning sample	# of samples
<i>Class D</i>	tapping sound of cracked wall	544
<i>Class C-1</i>	tapping sound of the clean wall which is shared with the next room	675
<i>Class C-2</i>	tapping sound of the clean wall fixed with metal plates from behind	260
<i>Class C-3</i>	tapping sound of the clean wall in front of pipes space	259

next room. *Class C-2* was that of the walls fixed by metal plates from behind. *Class C-3* was that of the walls in front of pipes space.

Four classifiers were created respectively for classifying one class from the others. Each class was detected by the results of these four classifiers based on the *One-versus-Rest* method, which is widely used to apply binary classifier to multi classification. The parameters of each classifier were set as the same with those of the experiment described in Section III-A

2) *Experimental Result*: Tapping each small area thirty times, a ratio of areas detected as defects (*Class D*) was calculated. The result is shown in Fig. 11. The XY coordinates correspond to the location shown in Fig. 10(b). The shades of colors show the defect ratio calculated as a percentage. A deeper color signifies that the area was more confidently classified as defective. The figure confirmed a larger defect ratio along the Y-axis at the middle of the X-axis direction (X=220mm–320mm). The result coincided with the location of cracks in the wall shown in Fig. 10(b). The effectiveness of the proposed methodology for wall crack detection was demonstrated.

The results of the other classes (*Class C-1*, *C-2*, *C-3*) are shown in Fig. 12(a), (b), (c), respectively. The XY coordinates and the meaning of color depth are the same as Fig. 11. For example, the result of Fig. 12(b) indicates that metal plates exist at top and bottom region (about Y=0mm–

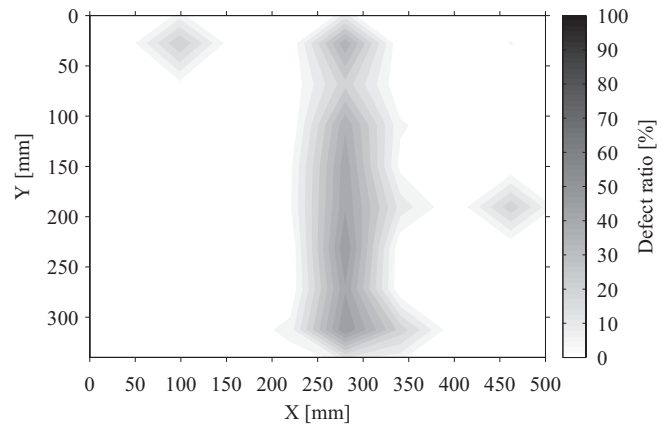


Fig. 11. *Class D*: Result of defect detection on a gypsum wall.

100mm, 250mm–340mm) of right-half side. The ground truth which was confirmed by visual inspection from behind the wall is shown in Fig. 12(d). The results of detection by classifiers well coincided with the real locations of the structures. The results confirmed that structures behind the wall can be detected using proposed methodology.

IV. CONCLUSION

In this paper, we proposed an automated diagnostic methodology for inspection work based on STFT and Adaboost using acoustic signals in the hammering test. In experiments of crack detection, the classifier was able to detect defects precisely. The results also confirmed that the methodology is applicable to different methods of hammering tests: *rubbing* and *tapping*. The hammering test is a highly convenient method that can be executed easily and rapidly. Moreover, our proposed system has benefits such as the high-speed diagnostic process, which can be finished in 6 ms on average, in addition to a compact apparatus and low cost of components. In automating a human walk-around check by robots, these advantages are effective from aspects of diagnostic accuracy, ease of installation, and cost suppression.

Several points must be considered in future research: improving feature vectors by considering physical phenomena of hammering test, integration of multi-modal sensors for

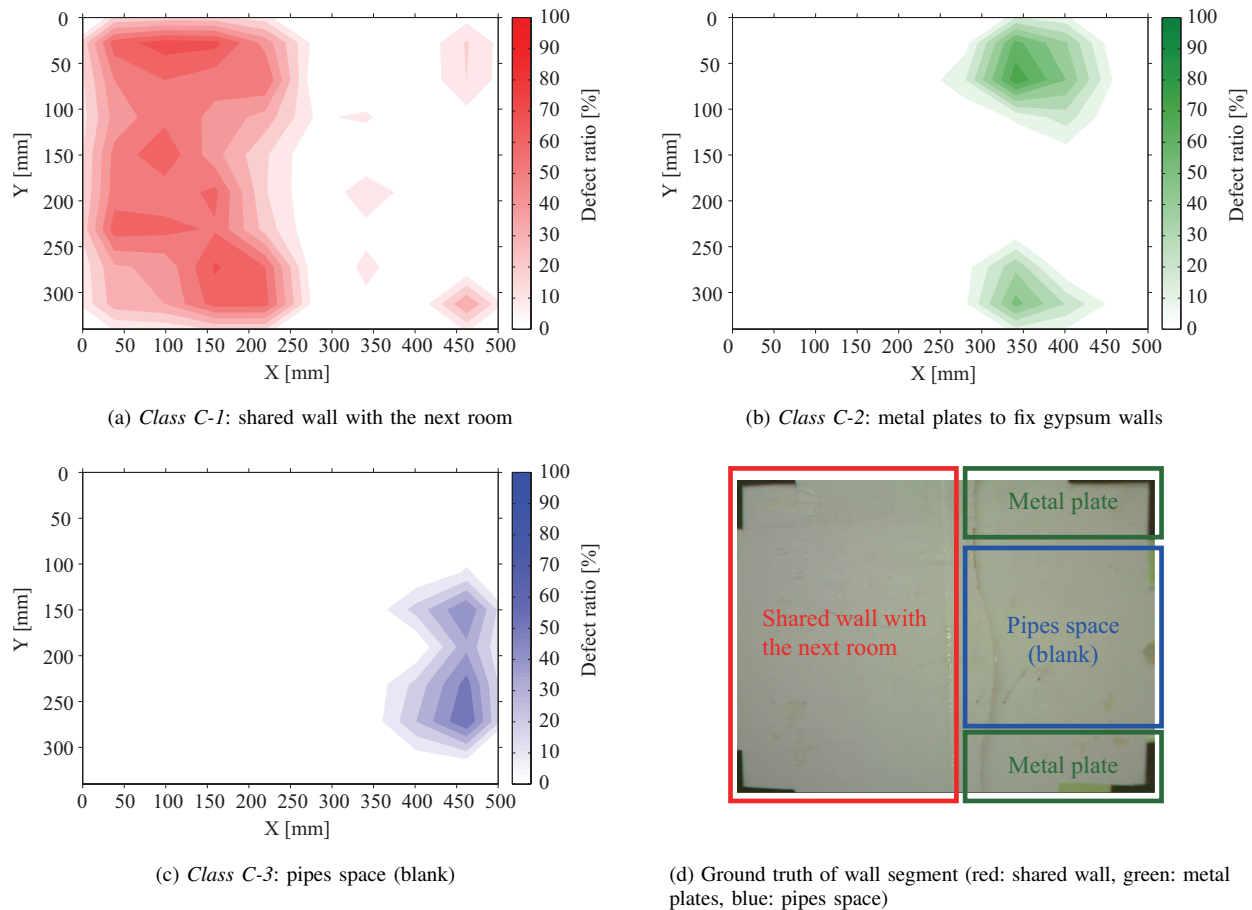


Fig. 12. Experimental result of structure detection behind the gypsum wall and the ground truth.

various inspections, collection of inspection data in a real field, and implementing this diagnosis system on robots.

ACKNOWLEDGMENT

This work was supported in part by Grant-in-Aid for JSPS Fellows 269039.

REFERENCES

- [1] Ryohei Takada, Naoki Oishi, "Priority Issues of Infrastructure Inspection and Maintenance Robot: A part of COCN 2012 project 'disaster response robot and its operational system'", Humanitarian Technology Conference (R10-HTC), 2013 IEEE Region 10, pp. 166–171, 2013.
- [2] Takeshi Suda, Atsushi Tabata, Jun Kawakami, Takatsugu Suzuki, "Development of an Impact Sound Diagnosis System for Tunnel Concrete Lining", Tunneling and Underground Space Technology, Vol. 19, Issue 4–5, pp. 328–329, 2004.
- [3] Fumihiro Inoue, Satoru Doi, Tatsuya Ishizaki, Yasuhiro Ikeda, Yutaka Ohta, "Study on Automated Inspection Robot and Quantitative Detection of Outer Tile Wall Exfoliation by Wavelet Analysis", Proceedings of International Conference on Control, Automation and Systems 2010, pp. 994–999, 2010.
- [4] Kenji Reichling, Michel Raupach, Herbert Wiggenhauser, Markus Stoppel, Gerd Dobmann, Jochen Kurz, "BETOSCAN-Robot Controlled Non-Destructive Diagnosis of Reinforced Concrete Decks", Non-Destructive Testing in Civil Engineering, 2009.
- [5] H. D. Cheng, Jim-Rong Chen, Chris Glazier, Y. G. Hu, "Novel Approach to Pavement Cracking Detection Based on Fuzzy Set Theory", Journal of Computing in Civil Engineering, Vol. 13, No. 4, pp. 270–280, 1999.
- [6] Atsushi Yamashita, Takahiro Hara, Toru Kaneko, "Inspection of Visible and Invisible Features of Objects with Image and Sound Signal Processing", Proceedings of the 2006 IEEE/RSJ International Conference on Intelligent Robots and Systems, pp. 3837–3842, 2006.
- [7] Takashi Onoda, Norihiko Ito, Hironobu Yamasaki, "Trouble Condition Sign Discovery Based on Support Vector Machines for Hydroelectric Power Plants", International Joint Conference on Neural Networks, pp. 2358–2365, 2009.
- [8] Shivprakash Iyer, Sunil K. Sinha, Bernhard R. Tittmann, Michael K. Pedrick, "Ultrasonic Signal Processing Methods for Detection of Defects in Concrete Pipes", Automation in Construction, Vol. 22, pp. 135–148, 2012.
- [9] Shiwei Ma, Tetsuya Sasaki, Etsuji Yoshihisa, Takashi Honda, "Time-Frequency Analysis of Ultrasonic Echoes and its Application to Nondestructive Evaluation of Thermal Damage of Steel", Research Reports of the National Institute of Industrial Safety, NIIS-RR-2002, 2003.
- [10] Mustapha Mjit, Pierre-Philippe J. Beaujean, David J. Vendittis, "Comparison of Fault Detection Techniques for an Ocean Turbine", Annual Conference of the Prognostics and Health Management Society, pp. 123–133, 2011.
- [11] Marco Cocconcelli, Radoslaw Zimroz, Riccardo Rubini, Walter Bartelmus, "STFT Based Approach for Ball Bearing Fault Detection in A Varying Speed Motor", Condition Monitoring of Machinery in Non-Stationary Operations, Springer Berlin Heidelberg, pp. 41–50, 2012.
- [12] Yoav Freund and Robert E. Schapire, "A Decision-Theoretic Generalization of on-Line Learning and an Application to Boosting", Journal of Computer and System Sciences, Vol. 55, Issue 1, pp. 119–139, 1997.
- [13] Paul Viola and Michael Jones, "Robust Real-time Face Detection", International Journal of Computer Vision, Vol. 57, No. 2, 2004, pp. 137–154, 2004.